Excited-state proton transfer in 1-naphthol/ammonia clusters

M. F. Hineman, G. A. Brucker, D. F. Kelley, and E. R. Bernstein

Citation: The Journal of Chemical Physics **97**, 3341 (1992); doi: 10.1063/1.462971
View online: http://dx.doi.org/10.1063/1.462971
View Table of Contents: http://aip.scitation.org/toc/jcp/97/5
Published by the American Institute of Physics

Excited-state proton transfer in 1-naphthol/ammonia clusters

M. F. Hineman, G. A. Brucker,[a] D. F. Kelley, and E. R. Bernstein
Colorado State University, Department of Chemistry, Fort Collins, Colorado 80523

(Received 31 January 1992; accepted 26 May 1992)

Excited-state proton transfer dynamics are reported for the 1-naphthol$(NH_3)_n$ cluster system for $n=3$ and 4. Picosecond time- and mass-resolved pump ($S_1 \leftarrow S_0$)–probe ($I \leftarrow S_1$) experiments demonstrate the following results: (1) excited-state proton transfer occurs for $n=3$ and 4 clusters only; (2) for $n=5$ clusters the proton is transferred in the ground state and for $n=2$ clusters no proton transfer can be observed; (3) the proton transfer time in the $n=3$ cluster at the 0_0^0 transition is ca. 60 ps; (4) this time is reduced to ca. 40 ps and ca. 10 ps for 800 and 1400 cm^{-1} of vibrational energy in S_1, respectively; (5) for the $n=4$ clusters these times are approximately 70, 70, and 30 ps, for 0, 800, and 1400 cm^{-1} of vibrational energy in S_1, respectively; (6) both $n=3$ and 4 clusters exhibit a second low-amplitude decay component, which is about an order of magnitude slower than the initial decay; and (7) 1-naphthol-$d_1(ND_3)_n$ clusters have a greatly reduced rate constant for the excited-state proton transfer dynamics. These observations are well fit and explained by a simple statistical/barrier penetration model involving proton tunneling and the effect of van der Waals vibrations on the height and width of the barrier to proton transfer.

I. INTRODUCTION

Proton transfer is a central mechanistic and kinetic step in a large number of important reactions. Reactions involving proton transfer are strongly affected by the surrounding solvent: several studies of proton transfer mechanisms and dynamics in bulk condensed phases have appeared encompassing solvent, *p*H, and isotope effects.[1,2] In these studies the effects observed can be related to the bulk properties of the solvent. The individual effects of solvent molecules and solute–solvent geometry can also be explored in the condensed phases through the study of matrix-isolated clusters.[3] Gas-phase studies of clusters and cluster chemistry are also now appearing,[4–9] which can provide additional microscopic details of the solute–solvent structure and the effect of the solvent on solute–solvent chemistry (e.g., proton transfer). These latter studies are of both a static[4–7] and dynamic[8,9] nature. Two very sensitive tests of the mechanism of a proton transfer reaction are the hydrogen/deuterium isotope effect and the effect of vibrational excitation within the solute–solvent cluster on the reaction rate constant. Proton transfer reactions in gas-phase clusters are not well explored partly because these latter two experiments have not been performed and partly due to other experimental difficulties. Studies to date suggest that the occurrence of proton transfer for phenol and 1-naphthol clustered with water and ammonia solvents is a function of cluster size and composition.[3–9]

This report is concerned with proton transfer in 1-naphthol/ammonia clusters; in particular, the effects of cluster size, vibrational state, and hydrogen/deuterium substitution [i.e., 1-naphthol-$d_1(ND_3)_n$ vs 1-naphthol-$h_1(NH_3)_n$] on the excited-state proton transfer dynamics are observed and modeled. Excited-state proton transfer is found to take place in these systems for clusters with three and four ammonia solvent molecules. The transfer rate increases for increased S_1 vibrational excitation, decreases for the deuterium-substituted clusters, and is independent of the wavelength of probe laser used to ionize the cluster for detection. A simple model involving proton tunneling is proposed which explains these observations nearly quantitatively.

II. EXPERIMENTAL PROCEDURES

1-Naphthol/ammonia clusters are formed in a seeded helium supersonic jet expansion. 1-Naphthol is purchased from Kodak and used without purification. For isotope effect studies the hydroxyl proton of 1-naphthol is exchanged with deuterium by dissolving 1-naphthol in anhydrous ether and washing the solution several times with D_2O. The ether and water layers are separated from one another and the ether is evaporated under vacuum. 1-Naphthol-OD (1-naphthol-d_1) crystals are recovered from this process.

1-Naphthol is placed in the sample compartment of a pulsed nozzle and heated to roughly 80 °C. The helium expansion gas is maintained at 55 psi (gauge) and contains 0.05% to 0.1% ammonia. The molecular beam enters the ionization region of a resonance-enhanced, two-photon ionization, mass spectrometer.[10] The clusters formed in the expansion are detected by a two-color pump–probe ionization scheme involving the transitions $I \leftarrow S_1 \leftarrow S_0$. Time-resolved signals for the S_1-state proton transfer reaction are obtained by varying the time delay between the pump and probe beams.

The laser system used for this study is shown in Fig. 1. A mode-locked, frequency-doubled, cw, Nd:YAG laser (Spectra Physics model 3800S) synchronously pumps two dye lasers (Spectra Physics model 3500). Approximately 10% of the remaining 1064 nm beam is used to seed a

[a]Present address: Chemistry Department, University of Southern California, Los Angeles, CA 90089.

 0021-9606/92/173341-07$006.00

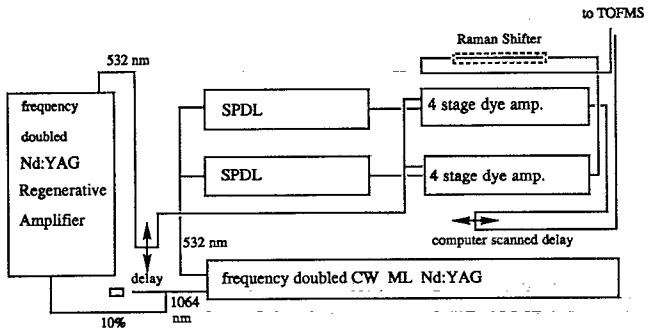

FIG. 1. The picosecond laser apparatus, SPDL denotes the synchronously pumped dye laser.

Nd:YAG regenerative amplifier (Spectra Physics model GCR-3A), the output of which when frequency doubled provides up to 40 mJ of 532 nm light in a 50 ps pulse at a repetition frequency of 10 Hz. This pulse is split 50/50 and pumps two homebuilt four-stage dye amplifier trains. The outputs of the amplifier trains are tunable pulses of ~5–8 ps duration with energies of 1–2 mJ. These pulses are frequency doubled in type-I KDP crystals to give tunable UV radiation with an intensity of a few hundred μJ/pulse. The UV pulses can be Stokes Raman shifted with nearly 30% efficiency in CH_4 to extend the accessible wavelength range of the system. Either one of the beams can be delayed with respect to the other using a computer-controlled, stepper-motor driven, linear motion stage.

Data acquisition is accomplished by setting an integrator gate on the appropriate time of flight for the ion of interest. The output of the integrator is sent to an analog-to-digital converter interfaced to the computer which controls the delay stage.

The excitation laser uses kiton red dye to give excitation energies, after frequency doubling, in the region from 30 800 to 32 500 cm^{-1}. The amplifier train employs either DCM or R640 as the gain medium. The ionization laser contains DCM and is amplified by either DCM or LDS 698 and frequency doubled. The ionization energy used for most experiments is in the range from 28 500 to 29 500 cm^{-1}. The ionization laser wavelength can be Stokes shifted (2914 cm^{-1}) by focusing the beam into a cell containing 120 psi of CH_4, permitting formation of the cluster ion with lower vibrational energy. The excitation laser pulse energy is kept below 20 μJ/pulse for all experiments, while the ionization laser pulse energy is maintained at 100–200 μJ/pulse. The pulse width of the amplified dye beams can be determined by autocorrelating or cross correlating the amplified beams using the delay stage and a KDP doubling crystal. For experiments requiring Raman-shifted beams, the dye amplifiers are run at high gain generating 350–400 μJ/pulse of frequency-doubled dye laser energy and resulting in 90–100 μJ/pulse in the Raman-shifted beam. Such high gain in the amplifier chain broadens the ionization laser pulse by a factor of ~3 to ca. 20 ps.

III. RESULTS

A. Spectroscopy

The steady-state excitation and ionization spectra of 1-naphthol/ammonia clusters have been reported.[4,5(a)] These spectra provide the necessary excitation and ionization energies for the clusters of interest as a function of cluster size. The 1-naphthol$(NH_3)_{1,2}$ clusters display sharp transitions that are red shifted from the bare molecule 1-naphthol origin (31 458 cm^{-1}) by 240 and 350 cm^{-1}, respectively. The $n=3$ clusters possess both sharp and broad features near their origin transitions, both of which are further red shifted from the bare molecule origin. The $n=4$ clusters have only broad spectra still further red shifted from the 1-naphthol origin. The $n=5$ cluster shows an anomalously large (1000 cm^{-1}) redshift relative the bare molecule 0_0^0.

The ion appearance potentials for the $n=1$ and 2 ammonia cluster ions are red shifted ~5000 cm^{-1} from that of the bare 1-naphthol molecule (62 600 cm^{-1}). The ion appearance potentials for the different geometries of the $n=3$ clusters are red shifted from that of 1-naphthol by ~5000 cm^{-1} for the cluster that does not undergo excited-state proton transfer and ~6600 cm^{-1} for the cluster that does undergo proton transfer.[5(a)] Clusters with $n \geqslant 4$ all have the same ionization appearance potential of ~55 900 cm^{-1}. The threshold for proton transfer as a function of cluster size for the 1-naphthol/ammonia system has thus been suggested to be that geometry of 1-naphthol$(NH_3)_3$ with the lower (like $n=4,...$) ionization appearance potential. The previous time-resolved studies[9] further substantiate this assignment.

1-naphthol is known to have two rotomers; syn and anti orientations of the hydroxyl group.[11] The anti conformer is the more stable and is the only one which has significant population in our supersonic jet expansion.[5(a)]

B. Dynamics—1-naphthol$(NH_3)_n$, $n=2$–5 origin

Time- and mass-resolved excitation ($1+1$, $I \leftarrow S_1 \leftarrow S_0$) data are collected on the $n=2$–5 clusters at the energies of their respective $S_1 \leftarrow S_0$ origin transitions. Only the $n=3$ and 4 clusters exhibit any time-dependent results. The time-resolved results are independent of ionization laser wavelength within the range from near the ion appearance threshold (25 000 plus 500 cm^{-1}) to 5000 cm^{-1} above the threshold. Naphthol$(NH_3)_n$ clusters with $n<3$ do not undergo proton transfer because the $(NH_3)_{1,2}$ moiety is not basic enough. Clusters with $n>4$ undergo proton transfer in the ground electronic state because $(NH_3)_{5,...}$ moieties are quite basic.[3–6] This interpretation is consistent with the large redshift in the $n=5$ cluster mass-resolved excitation spectrum.

Figure 2 shows a typical $1+1$ time- and mass-resolved ionization signal for 1-naphthol$(NH_3)_3$. The data are fit to a biexponential curve with $\tau_1=60$ and $\tau_2=500$ ps, and relative amplitudes of $A_2/A_1=0.3$. The instrument response function [~16 ps full width at half maximum (FWHM)] is obtained from the rise of the $n=1$ and 2 cluster signals. The decay time constants are fit with a

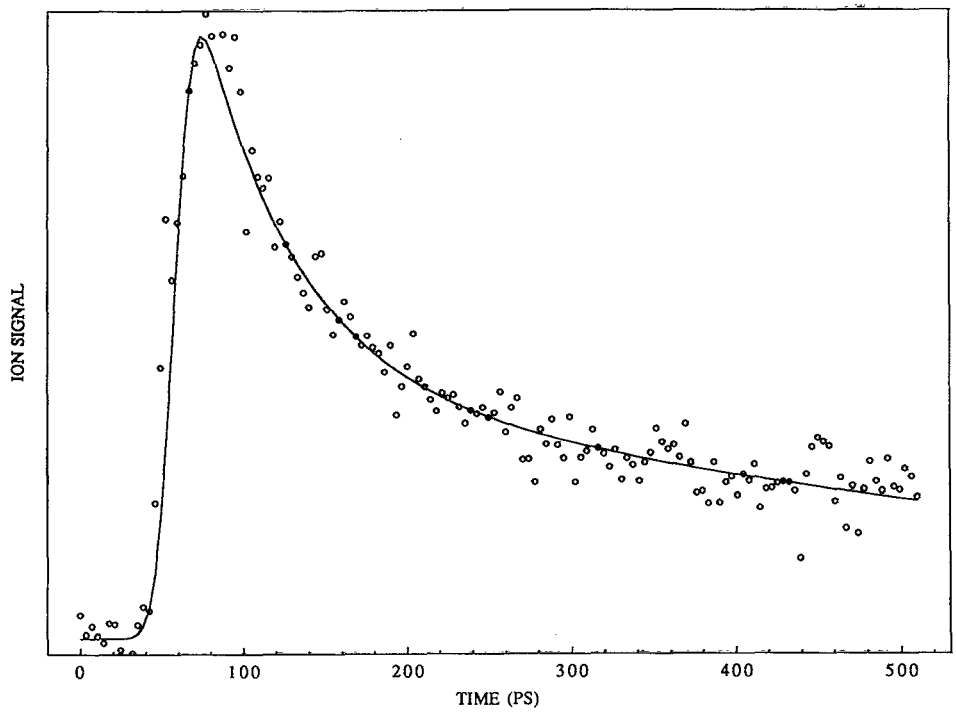

FIG. 2. Time-resolved 1+1 ionization signal scan of the 1-naphthol$(NH_3)_3$ cluster. Excitation energy, 31 100 cm^{-1}; ionization energy, 29 000 cm^{-1}. O, data; solid line, fit. The fit parameters are instrument limited rise followed by a biexponential decay $\tau_1=60$ ps and $\tau_2=500$ ps.

Levenberg–Marguardt algorithm.[12] The observed time dependence is assigned to the proton transfer process based on its cluster-size dependence and, as discussed below, isotope effect. The possibility of cluster fragmentation has been eliminated by careful searches for fragmentation products. The observed decay must therefore be due to a change in ionization cross section as the proton is transferred from 1-naphthol to ammonia in the S_1 state. The 1-naphthol$(NH_3)_4$ cluster decay times at the origin are similar: $\tau_1\sim 70$ ps and $\tau_2\sim 800$ ps, with a relative intensity ratio of $A_2/A_1\sim 1.0$. These data are summarized in Table I. As in the $n=3$ case, these decay time constants are independent of ionization energy from 500 to 4000 cm^{-1} above the ionization appearance threshold.

The analysis of the proton transfer dynamics of 1-naphthol$(NH_3)_{3,4}$ discussed below will focus on the proton transfer decay time τ_1. The second long decay time τ_2 can be attributed to either a cluster reorganization (which changes the $I\leftarrow S_1$ cross section) subsequent to the proton transfer event or a proton transfer associated with a cluster of different geometry.

TABLE I. Measured time constants for the nondeuterated clusters as a function of vibrational energy. Uncertainties (2σ) are given in parentheses.

Mass n	Excitation energy (cm^{-1})	τ_1 (ps)	τ_2 (ps)
3			
	31 100 (0_0^0)	57 (15)	440 (125)
	32 040	43 (11)	500 (74)
	32 490	12 (3)	119 (10)
4			
	30 800 (0_0^0)	71 (31)	800 (400)
	32 040	70 (30)	600 (100)
	32 490	33 (20)	1000 (500)

The proton transfer time ($\tau_1\sim 60$ ps) for the gas-phase 1-naphthol$(NH_3)_3$ cluster is a factor of 2 to 3 slower than the time observed for the argon matrix-isolated cluster (20–25 ps).[3(b)] The faster proton transfer rate in the matrix system can probably be attributed to polarizability of the surrounding environment. Matrix polarizability can have two effects on the proton transfer reaction: thermodynamic, in which the matrix stabilizes the ion pair products; and kinetic, in which the matrix reduces the height of the barrier to proton transfer.

The fact that the $n=3$ and $n=4$ clusters exhibit similar proton times suggests that the barriers to proton transfer in these clusters are similar. This result is somewhat surprising because $(NH_3)_4$ is expected to be more basic than $(NH_3)_3$: the increased ammonia cluster basicity would increase the proton transfer exothermicity and thus might be expected to lower the barrier to proton transfer. As the experimental rates demonstrate, this expectation is not confirmed. The likely explanation for the cluster reaction exothermicities not directly translating into cluster reaction rates is probably related to cluster structure. The $n=4$ cluster geometry may require significant rearrangement to reach the final equilibrium solvated proton structure. Thus, the exothermicities of the $n=3$ and $n=4$ cluster reactions prior to reorganization of the ammonia could be fairly similar, resulting in comparable barriers. Without detailed

TABLE II. Effect of deuteration on measured time constants as a function of vibrational energy.

Mass H/D	Excitation energy (cm^{-1})	τ_1 (ps)	τ_2 (ps)
H	31 100	57	440
D	31 100	>1000	...
H	32 490	12	119
D	32 490	75	>1000

knowledge of the cluster structure before and after proton transfer quantitative comparisons of the barrier heights in clusters of different sizes are difficult to make.

C. Dynamics—1-naphthol$(NH_3)_m$, $n=3,4$ vibronic transitions

Excitation of the 1-naphthol molecular vibrations in the S_1 state of the van der Waals cluster is observed to increase the proton transfer rate even though the O–H stretch motion itself is not excited, and is not energetically accessible. Specifically, if $\sim 900\ cm^{-1}$ of vibrational energy is placed in the $n=3$ cluster S_1 state the signal decay times become $\tau_1 \sim 40$ ps and $\tau_2 \sim 500$ ps. At $\sim 1400\ cm^{-1}$ of vibrational energy for the $n=3$ cluster in S_1, the decay times drop to $\tau_1 \sim 12$ ps and $\tau_2 \sim 120$ ps. For the $n=4$ cluster the decay times at $\sim 1250\ cm^{-1}$ of S_1 vibrational energy are $\tau_1 \sim 70$ ps and $\tau_2 \sim 600$ ps and at $\sim 1700\ cm^{-1}$ of S_1 vibrational energy the decay times become $\tau_1 \sim 30$ ps and $\tau_2 \sim 1000$ ps. These data are also summarized in Table I. The $n=4$ cluster signals are much weaker and have much larger error limits than the $n=3$ signals. Nonetheless, they still show that the $n=4$ cluster has a reduced τ_1 time with increasing vibrational energy and that the overall effect of vibrational energy is less than that observed in the $n=3$ cluster.

Even with up to $1700\ cm^{-1}$ of vibrational energy in S_1 and up to $4000\ cm^{-1}$ of vibrational energy in the cluster ions no fragmentation of 1-naphthol$(NH_3)_{3,4}$ is observed: we do not find $(NH_3)_mH^+$ signals or is any time dependence found in 1-naphthol$(NH_3)_{1,2}$ mass channels.

D. Dynamics—1-naphthol-$d_1(ND_3)_3$

Perhaps the most convincing demonstration that the observed time-dependent cluster ionization signals for 1-naphthol$(NH_3)_{3,4}$ are indeed due to S_1 excited-state proton transfer is a substantial deuterium isotope effect on the observed rates. Moreover, if the changes in decay times are large, one can expect tunneling to be a major contribution to the proton transfer mechanism.

The observed decay times τ_1 and τ_2 for the deuterated $n=3$ cluster at the origin and at $1400\ cm^{-1}$ of vibrational energy in S_1 are given in Table II. For the 1-naphthol-$d_1(ND_3)_3$ cluster excited to the $S_1 \leftarrow S_0$ 0_0^0, virtually no proton transfer is observed. At $1400\ cm^{-1}$ of vibrational energy the decay time τ_1 of the signal decreases to 75 ps, roughly a factor of 6 larger than observed in the 1-naphthol$(NH_3)_3$ cluster.

These results corroborate the proton transfer interpretation of the observed S_1 1-naphthol$(NH_3)_{3,4}$ decay times and additionally suggest a mechanism for this reaction which involves proton tunneling through a barrier. Similar results and conclusions obtain for the 0_0^0 studies of matrix-isolated 1-naphthol$(NH_3)_3$ clusters.[3(b)]

IV. DISCUSSION

In this section we present a model for calculating the proton transfer rate constants for van der Waals clusters. The model employed consists of three essential features: (1) the untransferred and the transferred structures are separated from one another by a potential-energy barrier which can be characterized by a width and a height;[3,13,14] (2) the barrier width and height are modulated by vibrational excitation of the intermolecular cluster modes;[15–18] and (3) vibrational energy is distributed statistically among the vibrational (van der Waals) modes.

Two vibrational coordinates take on special significance in this model. First, the reaction coordinate is taken to be the O–H stretch. The hydroxyl group is hydrogen bonded to the ammonia nitrogen, and the barrier to proton transfer is taken to be along this O–H···N reaction coordinate. Second, the O···N distance in this hydrogen bond is of central importance in determining the height and width of the proton transfer barrier. This distance can be modulated by excitation of the "diatomic" stretch mode, for which the 1-naphthol and $(NH_3)_3$ moieties are taken to be the "atoms." Excitation of the O···N stretch can dramatically affect the proton tunneling rate.[15–18] Numerical application of this model requires calculation of the proton tunneling rate for each quantum state of the diatomic stretch mode and calculation of the probability of occupation of each quantum state. These calculations are discussed below. Tunneling rates can be calculated as a function of the O···N separation based upon the WKB approximation for particle penetration through a barrier of assumed functional form.

The model potential surface for this system is presented in Fig. 3, in which the untransferred proton is bound in a well and the transferred proton is represented as a free particle. The curve in Fig. 3 thus represents the hydrogen stretch coordinate. This curve is taken to be an inverted parabola centered about the top of the barrier: its height and width are measured from the OH vibration zero-point energy. The proton transfer reaction is exothermic and the products are expected to have a high density of states: this justifies both the "free-particle" product description and the barrier penetration limit. Under these approximations, the tunneling rate constant for the proton transfer reaction reduces to the well-known expression[14]

$$k = \nu \exp\left[-\frac{a}{\hbar}\pi(2mE_h)^{1/2}\right], \tag{1}$$

in which ν is the zero-point frequency for the proton in the potential well, E_h is the height of the barrier, and a is the barrier half width at the zero-point energy position in the reactant well. This expression is derived from the WKB

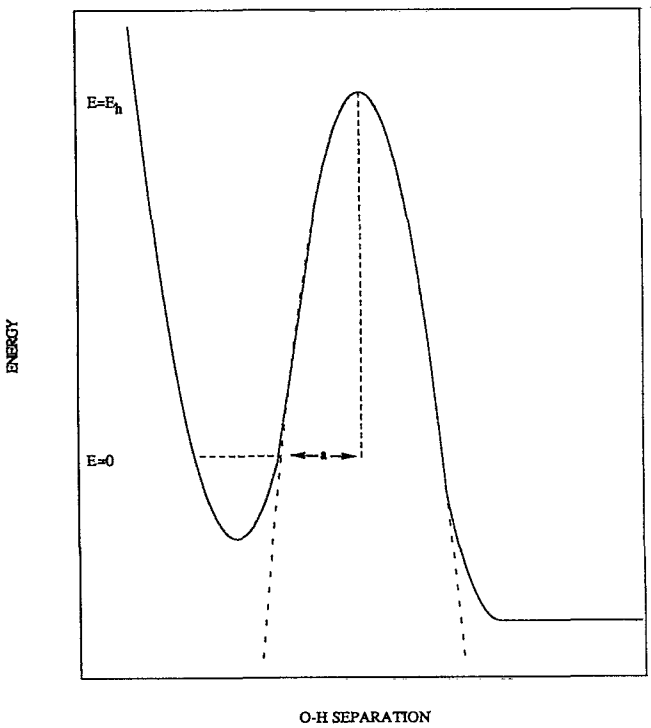

FIG. 3. Schematic diagram of the potential model used for proton transfer rate calculations. The dashed line is the parabolic barrier using parameters fit to origin $n=3$ data. The solid curve is the barrier model including a harmonic potential well with an OH vibrational energy of 3000 cm^{-1}. The well is centered at 1.0 Å. The other parameters for this model are $E_0=6500$ cm^{-1}, $a_0=0.2$ Å, and the van der Waals stretch energy is 110 cm^{-1} for 1-naphthol$(NH_3)_3$. See Eqs. (A1) and (A2) for the relation between E_h and a and their equilibrium values E_0 and a_0.

approximation to the wave function for particle penetration through a potential barrier. Assuming that this barrier is modulated by the stretching motion between the naphthol molecule and the ammonia cluster situated near the OH group, the barrier width and height is a function of the O···N distance.

Calculation of the proton transfer or barrier penetration rate as a function of the van der Waals vibrational excitation in the cluster requires an average of the rate constant of Eq. (1) over the wave function for the "diatomic" O···N distance. Thus,

$$k(v)=\langle\psi_v|k(a)|\psi_v\rangle, \tag{2}$$

in which ψ_v is taken to be a harmonic oscillator wave function, and v is the number of quanta in the O···N stretch mode.

The rate constant can be calculated for the O···N vibrational levels of cluster S_1 excitation using Eq. (2). Note that the vibrational energy in the cluster is never sufficient to excite the OH stretch either directly or indirectly. Calculation of ψ_v requires knowledge of the force constant and reduced mass of the "diatomic" O···N stretch. A reduced mass of 38 amu is calculated for the O···N stretch motion with naphthol and $(NH_3)_3$ taken as the two moieties in the "diatomic." The force constant is taken to be the same as that known for the phenol$(NH_3)_1$ system:[7,19] a vibrational energy of 110 cm^{-1} is calculated. Several other parameters are needed to evaluate Eq. (2). Specifically, the OH stretch in S_1 is chosen as 3000 cm^{-1}, assuming it is decreased from the bare phenol[20] by hydrogen bonding and the O···N distance in S_1 is taken to be the same as that recently determined for the excited-state naphthol$(NH_3)_1$ complex, 2.60 Å.[21] The equilibrium barrier half width at the zero-point level can be estimated for the classical turning points of the harmonic oscillator to be ~0.2 Å.

This model has only one adjustable parameter: the equilibrium barrier height, E_0. The vibrationless proton transfer rate for the $n=3$ cluster is fit to the observed rate of $(57\ ps)^{-1}$ to find a value for E_0 of 6500 cm^{-1}. The transfer rates as a function of the vibrational state can then be obtained. The details of the above calculations are given in the Appendix.

Cluster vibrational excitation in S_1 is generated by accessing vibrational states of 1-naphthol which are then assumed to undergo rapid relaxation [intracluster vibrational energy redistribution (IVR)] to the cluster van der Waals modes. Rapid naphthol to van der Waals mode IVR for the 1-naphthol$(NH_3)_{3,4}$ clusters is a good assumption based on the following two considerations: high cluster density of vibrational states, and known IVR cluster behavior for other cluster systems [e.g., aniline$(Ar)_1$, $(N_2)_1$, $(CH_4)_1$, and indole$(Ar)_{1,2}$ and $(CH_4)_1$ clusters].[22] The energy distribution in the van der Waals modes is then taken to be statistical and can be readily calculated. The probability that a specific van der Waals mode [in this case, the O···N "diatomic" stretch] is populated with v quanta is then calculated using the Marcus–Rice approximation[23]

$$P_v=\left(\frac{E-E_v}{E}\right)^{S-2}\Big/\sum_v\left(\frac{E-E_v}{E}\right)^{S-2}, \tag{3}$$

in which E is the vibrational energy in the cluster, E_v is the energy of the specific van der Waals mode, and S is the number of van der Waals modes for the cluster. The products of $k(v)$ and P_v for the modes of interest are summed to find the total transfer rate for a given S_1 vibrational energy and

$$k(E)=\sum_v P_v k(v). \tag{4}$$

Diatomic harmonic oscillator levels ($h\nu\sim110$ cm^{-1}) to $v=3$ are found to contribute to the observed rates with up to 1500 cm^{-1} of vibrational energy in the $n=3$ cluster. Table III presents the results of these calculations: agreement between the calculated transfer rates (τ_1^{-1}) based on the above model and the experimental results is excellent.

Isotopic substitution (H/D) affects the proton transfer rate in S_1 for the 1-naphthol$(NH_3)_3$ cluster in several ways: (1) the OD stretch has a zero-point energy which is much smaller than that of the OH stretch, and therefore both the barrier height and width increase; (2) the van der Waals vibrational reduced mass increases for $(ND_3)_3$, and thus the van der Waals vibrational energy decreases; and (3) the tunneling (proton) mass is doubled. The proton mass appears directly in the exponential [Eq. (1)] and as m increases the rate decreases. Increasing the barrier height

TABLE III. Comparison of barrier penetration model calculations with measured proton transfer time constants. See text for parameters used.

Mass n, H/D	Vibrational energy (cm^{-1})	τ_1 calculated[a] (ps)	τ_1 observed (ps)
3, H	0	57 fit	57
3, D	0	2140	>1000
3, H	940	28	43
3, H	1390	13	12
3, D	1390	180	75

[a] $E_0=6500\ cm^{-1}$, $a_0=0.2$ Å, $E(OH)=3000\ cm^{-1}$, $E(vdW)=110\ cm^{-1}$.

E_h and width a also decreases the rate. Decreasing the van der Waals vibrational energy also decreases the transfer rate but additionally increases the population of the particular mode. The model predicts that the deuteron transfer rate for the cluster should be small at the origin and should increase more quickly with vibrational energy than does the proton transfer rate for the protonated cluster. These results are clearly shown in Table III and represent excellent qualitative and quantitative agreement between the model and the experimental data. Both the trends and the details are well described: the effect of vibrational energy on the proton transfer rate of 1-naphthol$(NH_3)_3$ clusters is reproduced and the decrease of the isotope effect for the deuteron transfer rate of 1-naphthol-$d_1(ND_3)_3$ clusters as a function of vibrational energy is predicted as well.

Other methods of calculating the O···N separation-dependent proton transfer rates, such as a Fermi golden rule approach,[15] can also be employed. In this approach, two harmonic potential wells (e.g., O–H···N and O···H–N) are considered to be coupled by an intermolecular term in the Hamiltonian. Inclusion of the van der Waals modes into this approximation involves integration of the coupling term over the proton and van der Waals mode wave functions for all initial and final states populated at a given temperature of the system. Such a procedure requires the reaction exothermicity and a functional form for the variation of the coupling as a function of well separation. In the present study we employ the barrier penetration approach: this approach is calculationally straightforward and leads to a clear qualitative physical picture of the proton transfer process.

V. CONCLUSIONS

Excited-state proton rates are measured and modeled for 1-naphthol$(NH_3)_n$, $n=2$, 3, 4, 5, clusters as a function of vibrational energy in the S_1 state and as a function of hydrogen/deuterium isotope substitution. These rates are summarized in Tables I–III.

Proton transfer occurs for $n=3$ and 4 clusters in the S_1 state and is suggested to occur in the S_0 state for $n\geqslant 5$. No transfer is found for $n<3$ clusters. Substitution of deuterium for hydrogen in these clusters [i.e., 1-naphthol-$d_1(ND_3)_3$] has dramatic effects on the observed transfer rates. At the origin of the $S_1\leftarrow S_0$ transition the kinetic isotope effect is at least a factor of 20 (D^+ transfer is slower than H^+ transfer) but at an energy of 1400 cm^{-1} the kinetic isotope effect is about a factor of 6. The proposed model for proton transfer in these clusters equates proton transfer with a simple barrier penetration problem. The height and width of the barrier are modulated by vibrational energy in the cluster intermolecular van der Waals modes. The deuterium isotope effect is related to the OD zero-point energy, the reduced van der Waals mode energy for the 1-naphthol-$d_1(ND_3)_3$ cluster, and the H/D masses. The general trends and detailed rates observed are well described by the model.

ACKNOWLEDGMENTS

This work was supported by grants from the NSF and ONR. The authors would also like to thank Dr. D. W. Pratt for preprints of his work.

APPENDIX

In this Appendix we obtain expressions for the proton transfer barrier height and width as a function of the van der Waals vibrational displacements and derive equations for the proton barrier crossing rate constant as a function of the van der Waals vibrational level.

The potential used in this calculation is indicated schematically in Fig. 3. The barrier to proton tunneling is taken to be an inverted parabola with height E_h (measured from the zero point energy level) and half-width a. Hetero-atom motion changes the width of the barrier from its equilibrium value. With the assumption that the curvature of the parabola remains constant, hetero-atom motion also changes the barrier height, as given by

$$E_h=E_0(1+x/2a_0)^2, \tag{A1}$$

in which E_0 is the barrier height at equilibrium O···N separation and x is the deviation of this separation from its equilibrium value. The variation of the barrier half width is

$$a=a_0(1+x/2a_0), \tag{A2}$$

in which a_0 is the barrier half width at the equilibrium separation. The effect of small asymmetries of the size expected for this system ($\leqslant 5000\ cm^{-1}$ of minimum energy difference between the two wells and frequency differences of 10% to 20%) on the accuracy of Eq. (A1) is sufficiently small ($<5\%$) to ignore. Substitution of these into Eq. (1) gives

$$k(x)=\nu\exp\left[-\frac{(2mE_0)^{1/2}}{\hbar}\pi a_0\left(1+\frac{x}{2a_0}\right)^2\right]. \tag{A3}$$

Equation (A3) may now be substituted into Eq. (2) and, assuming harmonic oscillator wave functions for the O···N vibration, the integrals which must then be performed are of the form

$$\int_{-\infty}^{+\infty} x^n\exp(-px^2+2qx)dx. \tag{A4}$$

Equation (A4) has the value[24]

$$\frac{1}{2^{n-1}p}\left(\frac{\pi}{p}\right)^{1/2}\frac{d^{n-1}}{dq^{n-1}}\left(q\exp\frac{q^2}{p}\right). \tag{A5}$$

The rate constants calculated for harmonic oscillator wave functions up to $v=3$ using the substitutions,

$$\beta=\exp-\sqrt{2mE_0}\,\frac{\pi a_0}{\hbar},$$

$$q=-\frac{\pi}{2\hbar}\sqrt{2mE_0}, \tag{A6}$$

$$p=\frac{\mu\omega}{\hbar}+\frac{\pi}{4a_0\hbar}\sqrt{2mE_0},$$

in which m is the proton mass, μ is the van der Waals stretch reduced mass, and ω is the van der Waals stretch frequency are expressed as follows.

For $v=0$,

$$k(v=0)=\nu\beta\left(\frac{\mu\omega}{\hbar p}\right)^{1/2}\exp\left(\frac{q^2}{p}\right). \tag{A7}$$

For $v=1$,

$$k(v=1)=\nu\beta\left(\frac{\mu\omega}{\hbar p}\right)^{3/2}\left(1+\frac{2q^2}{p}\right)\exp\left(\frac{q^2}{p}\right). \tag{A8}$$

For $v=2$,

$$k(v=2)=\frac{\nu\beta}{2}\left(\frac{\mu\omega}{\hbar p}\right)^{1/2}\left[1-\frac{\mu\omega}{2\hbar p}\left(1+\frac{2q^2}{p}\right)+\left(\frac{\mu\omega}{\hbar}\right)^2\frac{1}{2p}\left(\frac{6}{p}+\frac{12q^2}{p^2}+\frac{8q^4}{p^3}\right)\right]\exp\left(\frac{q^2}{p}\right). \tag{A9}$$

For $v=3$,

$$k(v=3)=\frac{\nu\beta}{3}\left(\frac{\mu\omega}{\hbar p}\right)^{3/2}\left[\frac{9}{2}\left(1+2\frac{q^2}{p}\right)-\frac{3}{2}\left(\frac{\mu\omega}{\hbar}\right)\times\left(\frac{6}{p}+12\frac{q^2}{p^2}+8\frac{q^4}{p^3}\right)+\frac{1}{8}\left(\frac{\mu\omega}{\hbar}\right)^2\times\left(\frac{60}{p^2}+360\frac{q^2}{p^3}+240\frac{q^4}{p^4}+32\frac{q^6}{p^5}\right)\right]\exp\left(\frac{q^2}{p}\right). \tag{A10}$$

Overall rates may then be evaluated using Eq. (4).

[1] S. P. Webb, L. A. Philips, S. W. Yeh, L. M. Tolbert, and J. H. Clark, J. Phys. Chem. **90**, 5154 (1986).

[2] E. W. Kosower and D. Huppert, Annu. Rev. Phys. Chem. **37**, 127 (1986).

[3] (a) T. C. Swinney and D. F. Kelley, J. Phys. Chem. **95**, 2430 (1991); (b) G. A. Brucker and D. F. Kelley, Chem. Phys. **136**, 213 (1989); (c) J. Phys. Chem. **93**, 5179 (1989); J. Chem. Phys. **90**, 5243 (1989); J. Phys. Chem. **92**, 3805 (1988); **91**, 2862 (1987); **91**, 2856 (1987); D. F. Kelley and G. A. Brucker, *Ultrafast Phenonomena V* (Springer, Berlin, 1986), p. 330.

[4] O. Cheshnovsky and S. Leutwyler, J. Chem. Phys. **88**, 4127 (1988).

[5] (a) S. K. Kim, S. Li, and E. R. Bernstein, J. Chem. Phys. **95**, 3119 (1991); (b) S. K. Kim, S. C. Hsu, S. Li, and E. R. Bernstein, *ibid.* **95**, 3290 (1991); S. Li and E. R. Bernstein, *ibid.* (submitted); J. A. Warren, E. R. Bernstein, and Jeffrey I. Seeman, *ibid.* **88**, 871 (1988); H. S. Im, V. H. Grassian, and E. R. Bernstein, J. Phys. Chem. **94**, 222 (1990).

[6] R. Knochenmuss and S. Leutwyler, J. Chem. Phys. **91**, 1268 (1989).

[7] C. Jouvet, C. Lardeux-Dedonder, M. Richanr-Viard, D. Solgadi, and A. Tramer, J. Phys. Chem. **94**, 5041 (1990).

[8] J. A. Syage and J. Steadman, J. Chem. Phys. **95**, 2497 (1991); J. Steadman and J. A. Syage, J. Am. Chem. Soc. **113**, 6786 (1991).

[9] J. J. Breen, L. W. Peng, D. M. Willberg, A. Heikal, P. Cong, and A. H. Zewail, J. Chem. Phys. **92**, 805 (1990).

[10] E. R. Bernstein, K. Law, and M. Schauer, J. Chem. Phys. **80**, 2007 (1984).

[11] J. R. Johnson, K. D. Jordan, D. F. Plusquellic, and D. W. Pratt, J. Chem. Phys. **93**, 2258 (1990).

[12] W. H. Press, B. P. Flannery, S. A. Teukolsky, and W. T. Vetterling, *Numerical Recipes* (Cambridge University, Cambridge, 1989).

[13] P. Kebarle, Annu. Rev. Phys. Chem. **28**, 445 (1977).

[14] R. P. Bell, *The Tunnel Effect in Chemistry* (Chapman-Hall, New York, 1980).

[15] W. Siebrand, T. A. Wildman, and M. Z. Zgierski, J. Am. Chem. Soc. **106**, 4083 (1984).

[16] W. R. McKinnon and C. M. Hurd, J. Phys. Chem. **87**, 1283 (1983).

[17] L. I. Trakhtenberg, V. L. Klochikhin, and S. Ya. Pshezhetsky, Chem. Phys. **69**, 121 (1982).

[18] D. C. Borgis, S. Lee, and J. T. Hynes, Chem. Phys. Lett. **162**, 19 (1989).

[19] N. Mikami, A. Okabe, and I. Suzuki, J. Phys. Chem. **92**, 1858 (1988).

[20] H. D. Bist, J. C. D. Brand, and D. R. Williams, J. Mol. Spectrosc. **21**, 76 (1966); **24**, 413 (1967).

[21] D. F. Plusquellic, X.-Q. Tan, and D. W. Pratt, J. Chem. Phys. (submitted).

[22] M. R. Nimlos, M. A. Young, E. R. Bernstein, and D. F. Kelley, J. Chem. Phys. **91**, 5286 (1989); M. Hineman, D. F. Kelley, and E. R. Bernstein, *ibid.* (in press); E. A. Outhouse, G. A. Bickel, D. R. Demmer, and S. C. Wallace, *ibid.* **95**, 6251 (1991).

[23] P. J. Robinson and K. A. Holbrook, *Unimolecular Reactions* (Wiley, New York, 1972).

[24] I. S. Gradshteyn and I. M. Ryzhik, *Table of Integrals, Series, and Products* (Academic, New York, 1980), Sec. 3.462, No. 2, p. 337.